

Propagation Characteristics of Finite-Width Conductor-Backed Coplanar Waveguides With Periodic Electromagnetic Bandgap Cells

Shau-Gang Mao, *Member, IEEE*, and Ming-Yi Chen

Abstract—Wave propagation along the finite-width conductor-backed coplanar waveguide (FW-CBCPW) with periodically loaded one-dimensional electromagnetic bandgap (EBG) cells proposed earlier by the authors is investigated theoretically and experimentally in this paper. The full-wave simulation in conjunction with Floquet's theorem is employed to find the dispersion diagram for characterizing the guided and leaky waves over a wide frequency range. For examining the guided-wave mode, the equivalent-circuit model is established to obtain the analytical formula of the Bloch impedance. The remarkable slow-wave factor 1.9–2.9 times higher than that of a conventional FW-CBCPW is presented. When operating frequency is sufficiently high, the leaky-wave mode is emitted so that the structure radiates in the backward direction. Good agreement among the results of the full-wave simulation, equivalent-circuit model, published data, and measurement supports the usefulness of the proposed full-wave simulation and also validates the analytical formula. By properly adjusting the circuit configuration, the periodic EBG structure with controllable propagation characteristics, which include the bandgap zone, the slow-wave factor, and the Bloch impedance for the guided wave, as well as the radiation main beam for the leaky wave, may be achieved.

Index Terms—Conductor-backed coplanar waveguide, electromagnetic bandgap (EBG), periodic structure.

I. INTRODUCTION

FROM ITS beginning more than 50 years ago, the field of periodic structures has been widely studied and has found many applications in a variety of microwave devices, such as traveling-wave tubes, filters, artificial dielectrics, phased-array antennas, and frequency-selective surfaces [2]–[5]. During the last few years, the periodic electromagnetic bandgap (EBG) structures, in which the solid-state bandgap concept is applied to the electromagnetic issue, have received significant attention due to their frequency-selective properties by loading micromaching holes or vias into the stratified substrates to create

the two-dimensional (2-D) or three-dimensional (3-D) periodic variations of materials [6], [7]. Many researchers note that EBG structures could be useful as novel TEM waveguides for feed structures [8], as high-*Q* resonators for filter design [9], as enhanced-gain antenna substrates [10], and as nonimaging antenna ground planes to reduce specific absorption rate (SAR) levels in cellular phone users [11].

The recent developments of the one-dimensional (1-D) EBG structures in planar technology, which are etched periodic patterns on the ground plane, signal strip of the microstrip lines, or coplanar waveguides, have inspired interest in the slow-wave propagation and forbidden frequency range [12]–[14]. However, these constructions require a suspending substrate so that the circuit cannot be mounted on a metal base to provide mechanical strength for a thin and fragile wafer and to act as a heat sink for circuits with active devices. In addition, the etched pattern on the signal strip is restricted to the dimension on the line itself so that the considerable slow-wave factor cannot be achieved. Moreover, excessive loss is generated due to the discontinuities that are mainly concentrated on the signal strip.

Several theoretical studies have recently been conducted to deal with the periodic EBG structures. The finite-difference time-domain method, finite-element method, and method of moments are applied to model the electromagnetic fields of the periodic structures into a single cell [15]–[18]. However, these methods are numerically intensive so that most of the research is still characterizing the entire periodic structures by utilizing full-wave simulation to obtain the scattering parameters, although costing comparatively much more memory and CPU time [14], [19]–[21].

In this paper, the propagation characteristics of the finite-width conductor-backed coplanar waveguide (FW-CBCPW) with periodically loaded EBG cells proposed by the authors [1] and shown in Fig. 1(a) is analyzed theoretically and experimentally. First, the dispersion diagram, which is also referred to as Brillouin diagram, is obtained by combining the commercial full-wave simulator and Floquet's theorem to model electromagnetic waves within a unit cell. Although the scattering parameters can be obtained by directly modeling electromagnetic fields through the whole periodic structures, such a method is inefficient and the physical mechanism involved in the EBG structure is still lacking. Therefore, knowledge of the guided- and leaky-wave characteristics for

Manuscript received October 15, 2001. This work was supported by the National Science Council of Taiwan, R.O.C., under Grant NSC 90-2219-E-212-003.

S.-G. Mao was with the Department of Electrical Engineering, Da-Yeh University, Changhua 515, Taiwan, R.O.C. He is now with the Department of Electronic Engineering, National Taipei University of Technology, Taipei 106, Taiwan, R.O.C.

M.-Y. Chen is with the Department of Electrical Engineering, Da-Yeh University, Changhua 515, Taiwan, R.O.C.

Digital Object Identifier 10.1109/TMTT.2002.804515

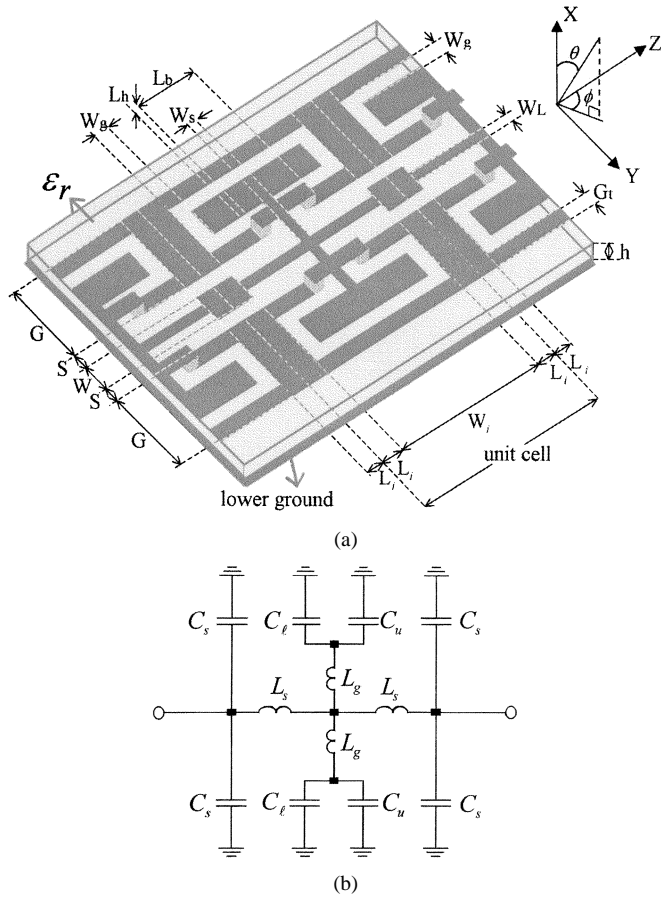


Fig. 1. 1-D EBG cell for FW-CBCPW. (a) Physical configuration. (b) Equivalent circuit. ($W_i = 12$ mm, $L_i = 1$ mm, $W = 3$ mm, $W_g = S = 0.5$ mm, $G = 5$ mm, $W_L = W_S = 0.6$ mm, $L_b = 3.6$ mm, $L_h = 2$ mm, $G_t = 1$ mm, $h = 1.6$ mm, and $\epsilon_r = 4.4$).

the periodic structures is essential and can be clearly illustrated in the dispersion diagram of the single EBG cell. Second, the equivalent-circuit model in conjunction with the Bloch wave analysis is used to find the analytical formula of the Bloch impedance. Third, the significant features of the guided-wave mode, i.e., the Bloch impedance, slow-wave factor, and bandgap zones, can be controlled well by properly designing the geometrical dimensions of the EBG cells. Finally, the leaky-wave characteristic, considered undesirable in the case of circuit design, is constructively utilized to establish the leaky-wave antenna.

II. THEORY

In this paper, the periodic structure consisting of a cascade connection of an infinite number of EBG cells separated by a FW-CBCPW, shown in Fig. 1(a), is investigated to find the guided- and leaky-wave characteristics. For theoretical modeling, the infinite periodic structure propagating in the z -direc-

tion is simplified to model the electromagnetic fields and the equivalent voltage and current waves within a unit cell by utilizing the full-wave simulation and equivalent-circuit model. Typical geometrical dimensions of the unit cell are also given in Fig. 1.

A. Full-Wave Simulation

To analyze the propagation characteristics of the FW-CBCPW with periodically loaded EBG cells, Floquet's theorem and the periodic boundary condition are incorporated into the full-wave approach to model the electromagnetic fields within a unit cell. The fields along the infinite periodic structure repeat at every terminal plane, except for a propagation factor $e^{-\gamma\Lambda}$, where $\Lambda = W_i + 2L_i$ is the length of a unit cell and $\gamma = \alpha + j\beta$ is the complex propagation constant in the z -direction. By using the commercial full-wave simulator, such as the moment-method-based Sonnet *em* and the finite-element solver Ansoft HFSS, the scattering matrix of the m th mode [S^m] propagating in the z -direction for a unit cell can be obtained; thus, γ can be determined by (1), shown at the bottom of this page [3]. Here, Z_{01} and Z_{02} are the impedance of ports 1 and 2, respectively, which, in this study, are $50\ \Omega$. Since the approach requires solving only one period of the periodic structure, the problem is small in size and short in executive time, even for relative complex structures.

B. Equivalent-Circuit Model

Fig. 1(b) depicts the equivalent-circuit model corresponding to the unit cell of the periodic structure shown in Fig. 1(a). The EBG cell is etched on both the signal strip and upper ground planes of the FW-CBCPW to produce arbitrary capacitance and inductance. The perforated patterns on the signal strip of the FW-CBCPW including a series narrow strip and step discontinuities are modeled by a series inductance L_S and two shunt capacitances C_S . The shunt narrow strip and the gap capacitance between the rectangular patch and upper/lower ground plane are corresponded to L_g and C_u/C_ℓ , respectively. By applying the Bloch wave analysis to the equivalent network of the unit cell, the normalized Bloch impedance Z_B can be expressed as

$$Z_B = \sqrt{\frac{2Z_1Z_3 + Z_1^2}{1 + \frac{1}{Z_2^2}(2Z_2Z_3 + 2Z_1Z_2 + 2Z_1Z_3 + Z_1^2)}} \quad (2)$$

where

$$\begin{aligned} Z_1 &= j\omega L_s \\ Z_2 &= \frac{1}{j2\omega C_s} \\ Z_3 &= j\omega \frac{L_g}{2} + \frac{1}{j\omega 2(C_\ell + C_u)}. \end{aligned}$$

$$\gamma = \frac{1}{\Lambda} \cosh^{-1} \left(\frac{\left[(1 + S_{11}^m)(1 - S_{22}^m) + S_{12}^m S_{21}^m \right] + \left(\frac{Z_{01}}{Z_{02}} \right) \left[(1 - S_{11}^m)(1 + S_{22}^m) + S_{12}^m S_{21}^m \right]}{4S_{21}^m} \right) \quad (1)$$

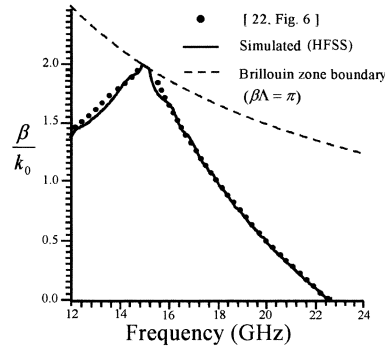


Fig. 2. Comparison of the normalized phase constant with the result of [22].

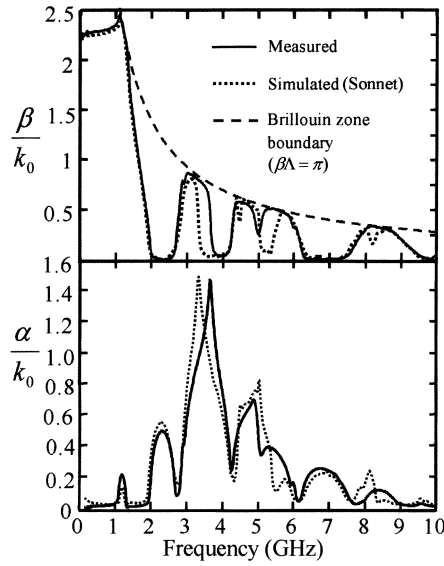


Fig. 3. Normalized phase constant and normalized attenuation constant of a single EBG cell with $W_i = 12$ mm and $L_i = 21$ mm based on full-wave simulation and measurement (for Figs. 3–9, the other dimensions are the same as in Fig. 1).

III. RESULTS AND DISCUSSION

The normalized phase constant β/k_0 , where k_0 is the free-space wavenumber based on the proposed full-wave simulation, is presented in Fig. 2 and is compared with the theoretical one from the volume integral-equation analysis for the fundamental guided- and leaky-wave modes of a grounded dielectric slab with 2-D periodic rectangular air blocks [22]. Good agreement among these results confirms the validity of the proposed full-wave approach for the periodic structure.

The normalized phase constant β/k_0 and normalized attenuation constant α/k_0 of a single EBG cell obtained from the full-wave simulation and measurement are also illustrated in Fig. 3 for comparison. All the circuits in this study are fabricated on a 1.6 mm-thick substrate ($\epsilon_r = 4.4$ and $\tan \delta = 0.022$) and have metallization thickness 0.02 mm and conductivity $\sigma = 5.8 \times 10^7$ S/m. By soldering air bridges at discontinuities to suppress higher order modes, this EBG structure ensures that the fundamental FW-CBCPW mode [23] is launched/received at input/output port. Note that the attenuation is presented at all frequencies when conductor and dielectric losses are included in the full-wave simulation. This lossy effect is neglected in the studies of [9] and [24]. Agreement among these results supports

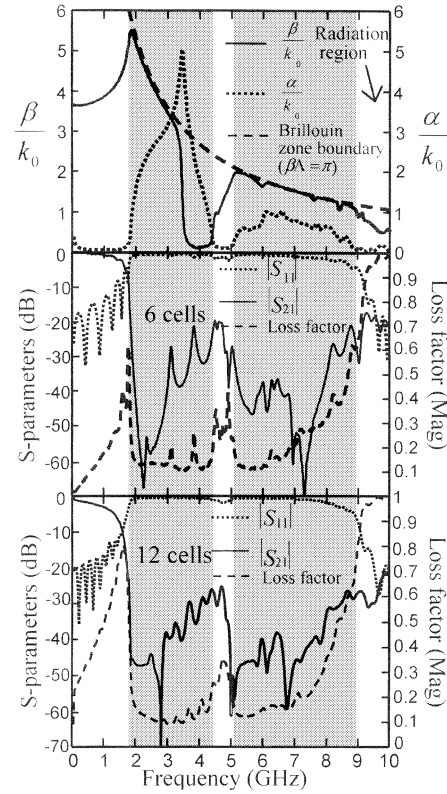


Fig. 4. Simulated dispersion diagram of one unit cell and the measured S -parameters of the periodic structure by cascading six and 12 EBG cells with $W_i = 12$ mm and $L_i = 1$ mm.

the usefulness of the proposed full-wave approach for the lossy EBG structures.

The simulated dispersion characteristic of one unit cell, as well as the measured S -parameters and loss factor $1 - |S_{11}|^2 - |S_{21}|^2$ of the periodic structure by cascading six and 12 EBG cells are shown in Fig. 4. In the following figures, the shaded regions in both the simulated dispersion diagram and the measured data represent that the electromagnetic wave is prohibited in the periodic structure. When β/k_0 is close to the Bragg condition ($\beta\Lambda = \pi$), the corresponding mode becomes a bound complex mode that is highly attenuating. The mode is no longer a propagating mode, but an evanescent mode that does not carry power. The frequency band within which the mode is complex is a guided-wave bandgap. Within the bandgap zone, since propagation is prohibited, there is considerable reflection; while out of the bandgap zone, the transmission is presented. The measured results for the 12-cell EBG structure are also included in Fig. 4. It is seen that the considerable rejection is presented in the stopband, when the cascading cells are increased.

When the frequency is sufficiently high up to 9 GHz, as shown in the simulated dispersion diagram of one EBG cell of Fig. 4, the periodic structure supports the fast-wave mode, i.e., $\beta/k_0 < 1$, with a small attenuation. Moreover, significant rise in the loss factor of the periodic structure is encountered due to radiation. The presence of this fast-wave mode, although causes larger power loss in the periodic structure, becomes necessary and provides useful information for leaky-wave antenna design. The measured co-polarized power gain pattern in the x - z -plane for the FW-CBCPW cascading 12 EBG cells

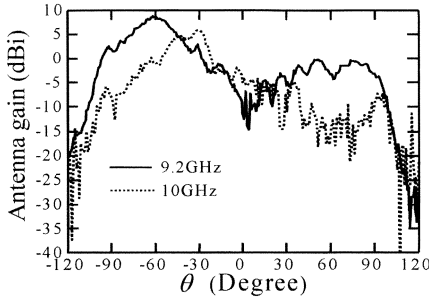


Fig. 5. Measured co-polarized power gain pattern at 9.2 and 10 GHz in the x - z -plane for the FW-CBCPW cascading 12 EBG cells with $W_i = 12$ mm and $L_i = 1$ mm.

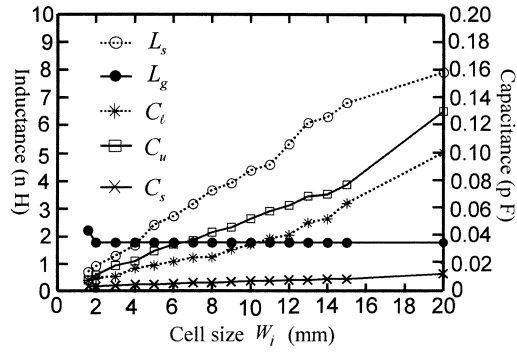


Fig. 6. Extracted inductances and capacitances of the equivalent-circuit model versus cell size W_i .

at 9.2 and 10 GHz is depicted in Fig. 5. The antenna is fed from the positive z -direction and the other end has a 50Ω match load to avoid reflection. The pattern is measured in an anechoic chamber with the ANTCOM near-field antenna measurement system. At 9.2 GHz, the main beam is directed at $\theta = -62^\circ$ with a gain of 8.9 dBi, i.e., 62° toward the backfire direction from the broadside, while at 10 GHz, the main-beam direction is -31° with a gain of 5.96 dBi. These results indicate that the fast-wave mode causes significant radiation in the backward direction and the frequency-scanning feature is also examined by changing frequency since the power flow is in the negative z -direction for this mode and the normalized leaky-wave phase constant decreases with frequency [25].

The results in Figs. 4 and 5 demonstrate that the guided- and leaky-wave characteristics of the FW-CBCPW with periodically loaded EBG cells depend principally on the fill factor, i.e., the ratio between the volume of material in the unit cell and the total volume of the unit cell, and can be predicted well by analyzing the dispersion diagram of one unit cell.

The circuit parameters for the derived equivalent circuit of a single EBG cell with $L_i = 0$ mm, shown in Fig. 1(b), are obtained by fitting the full-wave simulated data up to the frequency of the upper edge of the first bandgap zone. Fig. 6 plots the curves for the extracted inductance and capacitance parameters as a function of cell size W_i . Within the frequency range of interest, the shunt capacitance C_s slightly tends to increase and the series narrow strip inductance L_s and shunt gap capacitances C_u and C_t rapidly increase as W_i goes up. The shunt narrow strip inductance L_g is invariant because its physical length keeps constant during the variation of W_i . Each element in the circuit

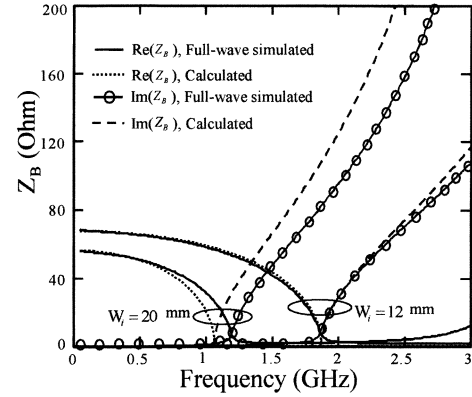


Fig. 7. Calculated and full-wave simulated Bloch impedance for a single-unit cell with $L_i = 0$ mm and W_i as parameters.

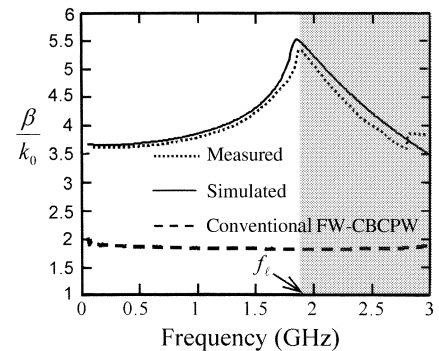


Fig. 8. Simulated and measured slow-wave factor of the EBG structure cascading 12 cells with $W_i = 12$ mm and $L_i = 1$ mm in comparison with the measured one of the conventional FW-CBCPW.

model has a definite connection with the physical dimension of the EBG cell such that the cutoff and stopband characteristics are easier to be controlled.

Fig. 7 shows the full-wave simulated Bloch impedance Z_B and the calculated one by (2) for a single-unit cell with $W_i = 12$ and 20 mm. In the first passband, Z_B is almost real, except for frequencies above the lower edge of the first stopband f_ℓ . Moreover, the proposed EBG cell can be matched to specific impedance over the frequency range of the first passband by adjusting the cell size W_i .

Fig. 8 depicts the simulated and measured β/k_0 (or slow-wave factor) of the EBG structure cascading 12 cells and, for comparison, the measured one of the conventional FW-CBCPW is also included. Note that the EBG structure exhibits a slow-wave characteristic and β/k_0 is 1.9–2.9 times larger than that of the conventional FW-CBCPW over the frequency range below f_ℓ . It is believed that the larger β/k_0 of the proposed structure can be easier obtained by enlarging the shunt rectangular patch in Fig. 1(a) without the need of finer fabrication process [14].

IV. CONCLUSION

The effect of periodicity for guided- and leaky-wave propagating in the FW-CBCPW with 1-D EBG cells has been investigated theoretically and experimentally in this paper. The full-wave approach utilizing the commercial field solver and

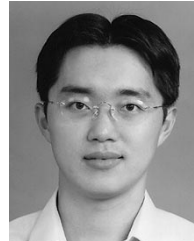
Floquet's theorem was proposed to model the periodic EBG structures efficiently. The dispersion diagram, which is a graphical representation of the dispersion relation for periodic structures, was found useful in describing the physical interpretation of the guiding and radiation behaviors. However, this diagram considers only for the direction of propagation that is modeled; propagation in the other direction must be modeled separately. The slow-wave propagation and backward-wave radiation for the periodic structure operating in the first passband and the radiation leaky region were demonstrated, respectively. To characterize the Bloch impedance, a simple equivalent-circuit model that consists of lumped-element inductors and capacitors was established to find the analytical formula. Experiments were also carried out to validate the proposed theory for the periodic EBG structure. The techniques presented in this paper may extend easily to characterize other complex periodic structures such as distributed-feedback lasers, log-periodic antennas, and artificial metallo-dielectric materials.

ACKNOWLEDGMENT

The authors wish to thank Prof. D.-C. Chang, Wireless Communication Research Center, Da-Yeh University, Taiwan, R.O.C., for providing access to their equipment for the measurement used in this paper.

REFERENCES

- [1] S.-G. Mao and M.-Y. Chen, "A novel periodic electromagnetic bandgap structure for finite-width conductor-backed coplanar waveguides," *IEEE Microwave Wireless Comp. Lett.*, vol. 11, pp. 261–263, June 2001.
- [2] C. Elach, "Wave in active and passive periodic structures: A review," *Proc. IEEE*, vol. 64, pp. 1666–1698, Dec. 1976.
- [3] R. E. Collin, *Field Theory of Guided Waves*, 2nd ed. New York: IEEE Press, 1991.
- [4] B. A. Munk, *Frequency Selective Surfaces*. New York: Wiley, 2000.
- [5] A. A. Oliner, "Periodic structures and photonic-band-gap terminology: Historical perspectives," in *29th Eur. Microwave Conf.*, vol. 3, Munich, Germany, Oct. 1999, pp. 295–298.
- [6] A. S. Barlevy and Y. Rahmat-Samii, "Characterization of electromagnetic band-gaps composed of multiple periodic tripods with interconnecting vias: Concepts, analysis, and design," *IEEE Trans. Antennas Propagat.*, vol. 49, pp. 343–353, Mar. 2001.
- [7] J. D. Joannopoulos, R. D. Meade, and J. N. Winn, *Photonic Crystals: Molding the Flow of Light*. Princeton, NJ: Princeton Univ. Press, 1995.
- [8] M. Belaid and K. Wu, "Quasi-optical power amplifier using TEM waveguide concept," in *IEEE MTT-S Int. Microwave Symp. Dig.*, vol. 3, May 2001, pp. 1835–1838.
- [9] W. J. Chappell, M. P. Little, and L. P. B. Katehi, "High isolation, planar filters using EBG substrates," *IEEE Microwave Wireless Comp. Lett.*, vol. 11, pp. 246–248, June 2001.
- [10] R. Cocciali, F. R. Yang, K. P. Ma, and T. Itoh, "Aperture-coupled patch-antenna on UC-PBG substrates," *IEEE Trans. Microwave Theory Tech.*, vol. 47, pp. 2123–2130, Nov. 1999.
- [11] R. F. J. Broas, D. F. Sievenpiper, and E. Yablonovitch, "A high-impedance ground plane applied to a cellphone handset geometry," *IEEE Trans. Microwave Theory Tech.*, vol. 49, pp. 1262–1265, July 2001.
- [12] D. Ahn, J. S. Park, C. S. Kim, J. Kim, Y. Qian, and T. Itoh, "A design of the low-pass filter using the novel microstrip defected ground structure," *IEEE Trans. Microwave Theory Tech.*, vol. 49, pp. 86–93, Jan. 2001.
- [13] Q. Xue, K. M. Shum, and C. H. Chan, "Novel oscillator incorporating a compact microstrip resonant cell," *IEEE Microwave Wireless Comp. Lett.*, vol. 11, pp. 202–204, May 2001.
- [14] J. Sor, Y. Qian, and T. Itoh, "A novel low-loss slow-wave CPW periodic structure for filter applications," in *IEEE MTT-S Int. Microwave Symp. Dig.*, vol. 1, May 2001, pp. 307–310.
- [15] L. Zhang and N. G. Alexopoulos, "Finite-element based techniques for the modeling of PBG materials," *Electromagnetics*, vol. 19, pp. 225–239, 1999.
- [16] H. Lee and J. Kim, "Modified Yee's cell for finite-difference time-domain modeling of periodic boundary guiding structure," in *IEEE MTT-S Int. Microwave Symp. Dig.*, vol. 2, May 2001, pp. 889–892.
- [17] R. Leone and H.-Y. D. Yang, "Design of surface-wave band-gaps for planar integrated circuits using multiple periodic metallic patch arrays," in *IEEE MTT-S Int. Microwave Symp. Dig.*, vol. 2, May 2001, pp. 1213–1216.
- [18] C.-K. Wu and C.-K. C. Tzuang, "Slow-wave propagation of microstrip consisting of electric-magnetic-electric (EME) composite metal strips," in *IEEE MTT-S Int. Microwave Symp. Dig.*, vol. 2, May 2001, pp. 727–730.
- [19] T. Akalin, M. A. G. Laso, T. Lopetegi, O. Vanbesien, M. Sorolla, and D. Lippens, "PBG-type microstrip filter with one- and two-sided patterns," *Microwave Opt. Technol. Lett.*, vol. 30, no. 1, pp. 69–72, 2001.
- [20] T.-Y. Yun and K. Chang, "Uniplanar one-dimensional photonic-bandgap structures and resonators," *IEEE Trans. Microwave Theory Tech.*, vol. 49, pp. 549–553, Mar. 2001.
- [21] Y. Chen, D. Bartzos, Y. Lu, E. Niver, M. E. Pilleux, M. Allahverdi, S. C. Danforth, and A. Safari, "Simulation, fabrication, and characterization of 3-D alumina photonic bandgap structures," *Microwave Opt. Technol. Lett.*, vol. 30, no. 5, pp. 305–307, 2001.
- [22] H.-Y. D. Yang, "Characteristics of guided and leaky waves on multi-layer thin-film structures with planar material gratings," *IEEE Trans. Microwave Theory Tech.*, vol. 45, pp. 428–435, Mar. 1997.
- [23] C.-C. Tien, C.-K. C. Tzuang, S. T. Peng, and C.-C. Chang, "Transmission characteristics of finite-width conductor-backed coplanar waveguide," *IEEE Trans. Microwave Theory Tech.*, vol. 41, pp. 1616–1624, Sept. 1993.
- [24] H.-Y. D. Yang, "Theory of microstrip lines on artificial periodic substrates," *IEEE Trans. Microwave Theory Tech.*, vol. 47, pp. 629–635, May 1999.
- [25] P. K. Potharazu and D. R. Jackson, "Analysis and design of a leaky-wave EMC dipole array," *IEEE Trans. Antennas Propagat.*, vol. 40, pp. 950–958, Aug. 1992.



Shau-Gang Mao (S'97–M'98) was born in Kaohsiung, Taiwan, R.O.C., in 1970. He received the B.S. degree in atmosphere science, and the M.S.E.E. and Ph.D. degrees in electrical engineering from the National Taiwan University, Taipei, Taiwan, R.O.C., in 1992, 1994, and 1998, respectively.

From October 1998 to July 2000, he fulfilled military service with the Department of Communication, Electronics, and Information, Coast Guard Administration, Executive Yuan, Taiwan, R.O.C., where he projected coastal surveillance and

communication systems. From August 2000 to January 2002, he was with the Department of Electrical Engineering, Da-Yeh University. Since February 2002, he has been an Assistant Professor with the Department of Electronic Engineering, National Taipei University of Technology, Taipei, Taiwan, R.O.C. His research interests include the design and development of millimeter-wave and microwave circuits and antennas.

Dr. Mao was the secretary of the IEEE Microwave Theory and Techniques Society (IEEE MTT-S), Taipei Chapter in 2001.



Ming-Yi Chen was born in Nantou, Taiwan, R.O.C., on September 11, 1977. He received the B.S.E.E. degree in electrical engineering from Da-Yeh University, Changhua, Taiwan, R.O.C., in 2000, and is currently working toward the M.S.E.E. degree in electrical engineering at Da-Yeh University.

His research interests include the design and analysis of microwave integrated circuits and devices.